Resonant Raman scattering of x rays: Evidence for K-M scattering

A. F. Kodre and S. M. Shafroth
Department of Physics and Astronomy, University of North Carolina, Chapel Hill, North Carolina 27514
(Received 25 May 1978)

Resonant Raman x-ray scattering on molybdenum was studied using a Mo-anode x-ray tube and a LiF crystal monochromator. Beside the usual resonant Raman peak corresponding to the fluorescent $K\alpha$ lines, another peak with a smaller energy loss was found. It is attributed to resonant Raman scattering with a final-state M-shell vacancy corresponding to the fluorescent $K\beta$ lines. Both contributions are shown to be independent of the scattering angle. Absolute cross sections have been determined and compared with theoretical predictions.

In 1974 Sparks[1] found a relatively strong inelastic component in scattering of Cu $K\alpha$ radiation from Ni, Cu, Zn, and Ge. The spectrum of the inelastically scattered radiation exhibited a sharp cutoff at the high-energy side, with a low-energy tail. The intensity of the scattered radiation decreased from Ni to Ge, i.e., as the energy of the K edge of the scatterer increased and got further from the energy of the incident photons. Bannet *et al.*[2,3] explained the effect with the resonant term in the Kramers-Heisenberg formula[4] with the final state consisting of an L-shell vacancy and an electron raised to the continuum, and with the intermediate state involving a virtual vacancy in the K shell of the target atom. Using synchrotron radiation as a tunable x-ray source Eisenberger *et al.*[5,6] investigated the transition of the resonant Raman scattering (RRS) into x-ray fluorescence as the energy of the incident photons was tuned across the K edge of the target. In the process the intermediate state develops into a real K-shell vacancy and the Raman peak in the spectrum of the scattered radiation goes continuously over into the characteristic $K\alpha$ lines of the scattering element.

In this letter, we report the evidence for another channel of the RRS in the vicinity of the K edge. It is attributed to RRS with an M-shell vacancy in the final state (K-M RRS). The scattering is related to the $K\beta$ lines of the target element in the same way as the usual (K-L) RRS is related to the $K\alpha$ lines. The finding confirms the view that the RRS is a multichannel process with every characteristic x-ray line having an RRS counterpart below its excitation threshold.

We investigated the RRS on metallic molybdenum and the neighboring elements employing the characteristic lines and the continuum radiation from a Mo-anode x-ray tube. A Bragg diffractometer with a LiF ($2d = 4.028$ Å) crystal was used as a monochromator of the incident radiation which had a linewidth of ~30 eV. The scattered radiation was analyzed with a Si (Li) detector of 30-mm^2 area and ~290-eV FWHM resolution for Mo $K\alpha$ lines. The detector had been calibrated for absolute efficiency.

The results of 120° scattering of near K-edge radiation on a thick Mo target are shown in the series of spectra in Fig. 1. The energy of the incident radiation is increasing upwards so that the evolution of the RRS peak can be seen. The lower-

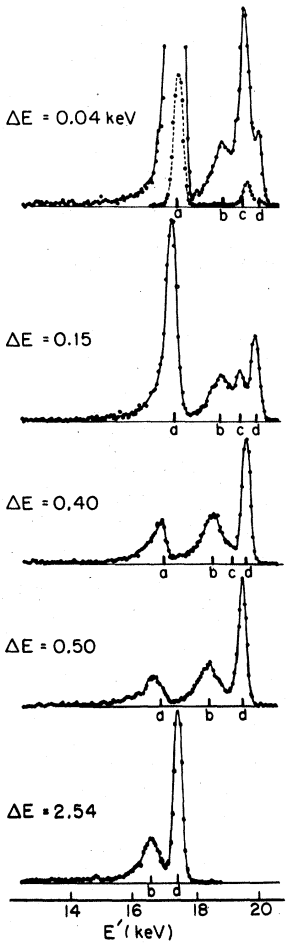

FIG. 1. Engergy spectra of x rays scattered at 120° from a thick Mo target in the order (from bottom to top) of increasing energy of the incident radiation shown by the labels $\Delta E = E_K - E$. Arrows a–d on the energy scale point to the calculated positions of the K-L RRS cutoff, the Compton peak, the K-M RRS cutoff, and the elastic peak, respectively. With the uppermost spectrum, a Mo fluorescence spectrum (dashed line—not to scale) is shown to provide a comparison for RRS peak positions. All spectra are normalized to the same incident beam intensity.

most spectrum is taken with the incident Mo $K\alpha_1$ line (~2.5 keV below the Mo K edge) where the RRS contribution is almost imperceptible in comparison to the Compton and the elastic scattering. The uppermost spectrum (taken with Mo $K\beta_2$ line, ~40 eV below the K edge) is compared to the Mo fluorescence spectrum (dotted line) to show that the strong RRS lines are not due to spurious fluorescence, being distinctly lower in energy.

In the last two spectra the evolution of the K-M RRS line between the elastic and the Compton scattering peak can be observed. Its nature has been deduced from its position in the spectrum and its resonant energy dependence. Such a contribution has been predicted by Bannet[3] but the experimental evidence for it has so far not been reported.

The term in the Kramers-Heisenberg formula relevant to RRS is

$$\frac{d\sigma}{d\Omega\, dE'} = C\left(\frac{E'}{E}\right)\frac{|\vec{p}\cdot\vec{\epsilon}'|_{fI}^2\,|\vec{p}\cdot\vec{\epsilon}|_{Ii}^2}{(E_I - E_i - E)^2 + \Gamma_I^2/4}\,, \tag{1}$$

where unprimed and primed quantities refer to the incident and the scattered photon, respectively, and the subscripts i, I, and f denote the initial, intermediate, and final states. r_0 and m, as usual, stand for the classical electron radius and electron mass, $\vec{p}$ is the momentum operator and $\vec{\epsilon}$ denote the polarization vectors of the photons. Numerical factors and atomic constants are contained in C.

Rewriting Eq. (1) for the specific case of the K-L RRS, we obtain

$$\frac{d\sigma}{dE'} = C'|M_{KL}|^2\frac{\sigma_K^{\text{photo}}(E_k)}{(E_{K\alpha} - E')^2 + \Gamma_K^2/4}\,, \tag{2}$$

where M_{KL} denotes the dipole matrix element for the $K\alpha$ transition and $\sigma_K^{\text{photo}}(E_k)$ is the K-shell photoelectric cross section expressed with the energy E_k of the electron ejected into the continuum, $E_k = E - E' - E_L$. The cutoff of σ_K^{photo} at $E_k = 0$ corresponds to the cutoff of the RRS spectrum at $E' = E - E_L$. It is evident from the theory that in this approximation the RRS is isotropic if the polarization of the scattered photon is not monitored. The experimental evidence for the RRS isotropy is given in Fig. 2.

Spectra of the scattered radiation at three different scattering angles are presented, all from Mo 40 eV below the edge. They are compared to the spectra obtained with the Mo target replaced by rhodium (dotted lines) where no RRS is present, to show the contributions of the elastic and the Compton scattering. While the latter two exhibit a strong angular dependence, the RRS in both peaks is apparently isotropic.

The absolute cross sections for the RRS on Mo

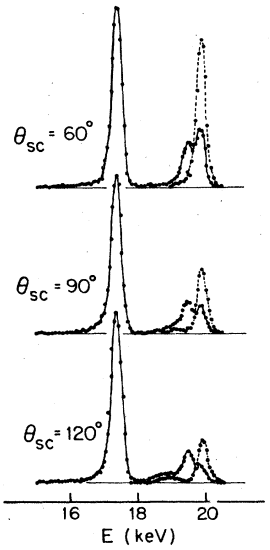

FIG. 2. Spectra of Mo $K\beta_2$ radiation ($\Delta E \sim 40$ eV) scattered from a thick Mo target at three different scattering angles. Dashed lines represent scattering from a Rh target in the same conditions, to show (with no RRS present) the angular dependence of the Compton and the elastic scattering. Spectra have not been corrected for a small effect of target absorption.

have been determined from the spectra in Fig. 1. Corrections for the counter efficiency, for the energy-dependent target absorption in the peak and for the finite summation interval of the peak were applied. In the reduction of the data the absorption coefficients from Weigele's compilation[7] were used. The results are shown in Table I.

The total RRS cross section is obtained from Eq. (2) by integrating from $E' = 0$ to the cutoff at $E' = E - E_L$. As the resonant region is limited to the immediate vicinity of the K edge, in all cases of interest $\Delta E = E_K - E \ll E_K$, we can disregard the slow E or E' dependence of factors on the right side of the Eq. (2) and take the value of the photoelectric cross section at the edge itself. On the other hand with the resolution of the experiment, $\Delta E \gg \Gamma_K$, so that we can drop Γ_K in the denominator. The result is

$$\sigma_{K\text{-}L}^{\text{RRS}} = \frac{C''}{\Delta E} + O(\ln \Delta E)\,. \tag{3}$$

TABLE I. Total cross sections for K-L and K-M RRS as a function of the incident photon energy, expressed as $\Delta E = E_K - E$ for Mo. Error intervals stem mainly from the uncertainties in peak separation and absolute efficiency calibration of the detector.

ΔE (keV)	$\sigma_{K\text{-}L}$ (b/atom)	$\sigma_{K\text{-}M}$ (b/atom)
0.544	8.5 ±2	
0.502	9 ±2	
0.395	12.5 ±2.5	
0.243	17 ±3	
0.225	21.5 ±3.5	3 ±1.5
0.128	40 ±3	4 ±2
0.104	45.5 ±5	5 ±2
0.038	180 ±20	34 ±6

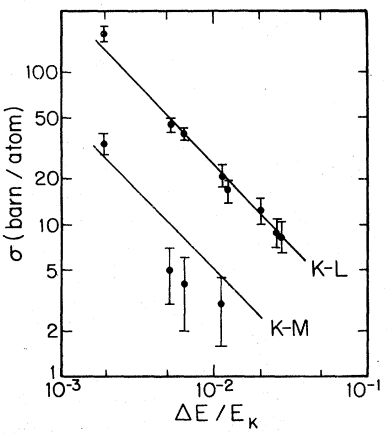

FIG. 3. The total K-L and K-M RRS cross sections for Mo. The experimental data from Table I are compared to the theoretical prediction $C''/\Delta E$ (solid curves). C''_{K-L} has been adjusted to a least-square fit of the experimental points. C''_{K-M} is obtained from C''_{K-L} by multiplying it with the $K\beta/K\alpha$ intensity ratio from Weigele (Ref. 7).

In Fig. 3 our results are compared to the above prediction. The K-L solid curve is a straight line with the slope -1 (in log-log plot) least-square fitted to the experimental points. The value 4.7 ± 0.5 keV b/atom for the constant C'' has been obtained from the fit. The K-M solid curve is not an independent fit: from the outlined theory it follows that the ratio of the scattering cross sections $\sigma^{\mathrm{RRS}}_{K-M}/\sigma^{\mathrm{RRS}}_{K-L}$ should be the same as the ratio of the intensities of the characteristic $K\beta$ and $K\alpha$ lines. The value 0.20 for that ratio given by Salem and Lee[8] for Mo, was used to construct the K-M prediction from the K-L fit.

As seen in Fig. 3, the trend of the K-L experimental data is in very good agreement with theory. The agreement of the K-M data is poorer, understandably so in view of uncertainty in resolving the K-M peak from the elastic peak and the Compton peak on both sides.

The Kramers-Heisenberg formula can as well be applied to x-ray fluorescence in the case $E > E_K$. In a similar approximation as above, the fluorescent cross section is given by

$$\sigma_K^{fl} = \omega_K \sigma_K^{\mathrm{photo}} = 2\pi C''/\Gamma_K \tag{4}$$

or

$$C'' = \frac{\sigma_K^{\mathrm{photo}}(\Gamma_K)_r}{2\pi}\,, \tag{4a}$$

where ω_K denotes the K-shell fluorescent yield and $(\Gamma_K)_r$ is the radiation width of the K shell. Equation (4) offers an independent way of checking the experimental value of C''. With $(\Gamma_K)_r \sim 3.5$ eV, as given by Krause[9] $C''_{\mathrm{theory}} = 6 \pm 1$ b keV/atom. In view of the low accuracy of the two values the agreement is satisfactory.

The existence of below threshold RRS precursors of characteristic x-ray lines, as demonstrated in our experiment, opens up an interesting field of studies in higher atomic shells, with the question of how much of the accompanying structure (satellites, intershell excitation) is retained below threshold. Besides, as shown in the above estimate, the study of RRS cross sections offers a method for direct determination of the level widths even in a low-resolution experiment.

ACKNOWLEDGMENT

We are grateful to the Material Sciences Group at the UNC Chapel Hill for permission to use their x-ray diffraction equipment for this work and to Dr. W. J. Thompson for very helpful comments on the manuscript. One of us (A.F.K.) was supported by a Fulbright fellowship from the University of Ljubljana, Yugoslavia. This work was supported in part by the U.S. Department of Energy.

[1] C. H. Sparks, Jr., Phys. Rev. Lett. 33, 262 (1974).
[2] Y. B. Bannet and I. Freund, Phys. Rev. Lett. 4, 372 (1975).
[3] Y. B. Bannet, D. C. Rapaport, and I. Freund, Phys. Rev. A 16, 2011 (1977).
[4] J. J. Sakurai, *Advanced Quantum Mechanics* (Addison-Wesley, Reading, Mass. 1967).
[5] P. Eisenberger, P. M. Platzmann, and H. Winnick, Phys. Rev. Lett. 36, 623 (1976).
[6] P. Eisenberger and P. M. Platzmann, Phys. Rev. B 13, 2377 (1976).
[7] W. J. Weigele, At. Data Tables 5, 51 (1973).
[8] S. J. Salem and P. L. Lee, At. Data Nucl. Data Tables 18, 233 (1976).
[9] M. Krause, J. Phys. Chem. Ref. Data (to be published).